Ultrafast Acoustic Phonon Ballistics in Semiconductor Heterostructures

J. J. Baumberg and D. A. Williams

Hitachi Cambridge Laboratory, Cavendish Laboratory, Madingley Road, Cambridge CB3 0HE, United Kingdom

K. Köhler

Fraunhofer-Institut fur Angewandte Festkörperphysik, 79108 Freiberg, Germany

Using a two-color ultrafast surface deflection spectroscopy, we demonstrate the time-resolved observation of acoustic phonon wave packets emitted from a single buried GaAs quantum well. A longitudinal acoustic phonon pulse is generated at a preselected depth within a highly confined region (≥ 10 nm thick) through the coherent nonequilibrium deformation potential which was previously unobserved in such structures. Subsequent detection with subpicosecond resolution at the surface resolves propagating high-wave-vector ballistic phonons and quasiballistic or "snake" phonons which subsequently merge into a quasidiffusive phonon pulse. [S0031-9007(97)03074-3]

Much is known about the energy relaxation of electrons in semiconductors, mainly due to the success of optical spectroscopies [1]. These can track both the hot carriers and the emitted optic phonons which absorb the bulk of the excess electron energy. Detailed studies have been driven by new theories which cope with the many-body electron-electron and electron-phonon interactions, and by growing numbers of technological applications. Recently developed ultrafast laser sources with pulse widths shorter than a single oscillation period of the optic phonon in semiconductors now enable *direct* temporal observation of the high-frequency long-wavelength lattice response [2]. However, in spite of this, only part of the system is ever being probed—the ultimate sink of the excess carrier energy is an acoustic phonon cascade. Initially, the acoustic phonons are highly nonthermal and coherent, undergoing both rapid energy conversion and elastic scattering off isotope and alloy fluctuations in the semiconductor [3]. Capabilities for probing THz acoustic phonons have improved in recent years, predominantly in metallic systems [4]. However, it has proved extremely difficult to access the early acoustic phonon distributions in semiconductors and the mechanisms that act to thermalize them.

Here, we introduce a complementary ultrafast optical technique which allows the study of acoustic pulses generated by exciting electrons and holes in a *single* GaAs quantum well (QW). Using pump and probe pulses of different wavelengths and an appropriately designed wafer cross section, carriers are selectively excited at a specific depth and the emitted phonons probed at the sample surface. In principle, this allows the emission processes to be discriminated and correlated with the carrier cooling dynamics. Using a single QW degrades the signal-to-noise ratio compared with analogous experiments on multiple wells or superlattices [5], but the discrimination of the phonon generation region in space and time, coupled with the detection at a preselected distance away, allows more concrete conclusions to be drawn from the observations.

Initial results show ballistic phonon wave packets emerging from the quantum well and a quasiballistic and quasi-diffusive phonon cascade from the GaAs substrate. These experiments open the way to the investigation of the generation, propagation, and detection of acoustic phonons in geometries relevant to heat transport and carrier relaxation in optoelectronic devices such as semiconductor lasers.

Samples grown by molecular beam epitaxy on (001) semi-insulating GaAs substrates contain single quantum wells of GaAs. These are placed at different depths relative to the sample surface, surrounded by $Al_{0.3}Ga_{0.7}As$ barrier layers, and capped at the surface with GaAs [Fig. 1(a)]. Growth was characterized by electron diffraction, and produced samples of high quality as shown by sub-meV photoluminescence linewidths with negligible Stokes shift. The 70 fs pulsed output of a mode-locked Ti:sapphire laser is tuned to excite electron-hole pairs in the lowest quantum-confined subband of the GaAs QWs

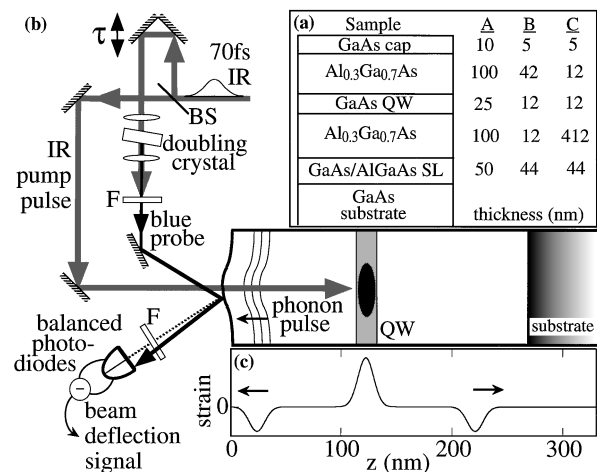| (a) Sample	A	B	C
GaAs cap	10	5	5
$Al_{0.3}Ga_{0.7}As$	100	42	12
GaAs QW	25	12	12
$Al_{0.3}Ga_{0.7}As$	100	12	412
GaAs/AlGaAs SL	50	44	44
GaAs substrate	thickness (nm)		

FIG. 1. (a) Vertical structure of wafers A, B, and C. (b) Schematic of the experimental arrangement (F = filter, BS = beam splitter, $T = 300$ K). (c) Calculated strain pulse dynamics after the QW is permanently stressed.

    0031-9007/97/78(17)/3358(4)$10.00   © 1997 The American Physical Society

with small excess carrier energies ($\sim$50 meV) to prevent intervalley scattering. A phonon wave packet is generated at the QW depth and propagates towards (and away from) the sample surface. In order to time resolve the arrival of the wave packet, a portion of the pulse train is split off into a probe beam which is time delayed and frequency doubled to produce blue pulses that are reflected from a focus overlapping that of the pump pulse. The phonon pulse causes a deformation of the sample surface and also changes the refractive index within the $\sim$16 nm skin depth penetrated by the probe photons. As depicted in Fig. 1(b), both these effects induce a deflection of the reflected beam if the focus is slightly displaced laterally with respect to the pump focus [6].

The reflected probe beam is incident on a balanced photodiode pair to record the deflection. Phase-sensitive detection of the residual current is sampled at the 372 kHz modulation frequency of the pump beam, and the resulting output digitized as the interpulse time delay is scanned at 8 Hz. The detection sensitivity is strongly enhanced by probing at the 3 eV GaAs absorption resonances termed E_1 and $E_1 + \Delta_1$ [7]. Efficient averaging, together with strong suppression of contaminating pump light using bandpass wavelength filters, allows the signal from *single* quantum wells to be isolated at carrier densities $\geq 10^{12}$ cm^{-2}.

Figure 2(a) shows the initial transient response for sample A at 295 K. Identification of the phonon-induced surface deflection signal is confirmed by translating the probe spot to the other side of the pump focus to generate the opposite deflection [Fig. 2(b)]. The surface phonon deflections vary little with the pump or probe polarizations relative to the crystal axes of the sample. The selectivity of the technique depends on the different interaction depths of the pump and probe pulses due to their widely separated photon energies. Probing instead with infrared pulses [Fig. 2(c)] yields a hundred times larger signal, from changes in refractive index induced by the reduction in oscillator strength of the QW, that masks any phonon contribution. Instead, cooling and recombination of the photoinjected carriers in the QW

are observed on the 100 ps time scale. Hence we are able to monitor both the electronic and acoustic phonon dynamics of a low-dimensional heterostructure within the same experimental arrangement.

The time-resolved phonon deflections shown in Figs. 2(a) and 2(b) display a small feature at zero delay composed of a subpicosecond spike in the response, followed by a persistent deflection. This response originates from the GaAs cap layer which is frequently ignored because of its proximity to surface states. The initial spike can arise from optical nonlinear mixing in the reduced symmetry of the surface layers or, alternatively, from photogenerated carriers being trapped on ultrafast time scales <1 ps. The subsequent long-lived deflection is caused by thermally and electronically induced variations in the cap layer refractive index. The initial response thus shows unusual sensitivity to the dynamics of the surface layers of GaAs.

After $\sim$20 ps, an oscillating transient is observed whose arrival time corresponds roughly to that expected from longitudinal acoustic (LA) phonons emitted in the buried QW ($v_s = 4930$ m s^{-1} in Al$_{0.3}$Ga$_{0.7}$As [8]), but which is preceded by a smaller amplitude pulse. Figure 3 shows the response for samples with different quantum well and substrate depths [Fig. 1(a)]. In each case, the arrival time expected for LA phonons from the quantum well and substrate layers is indicated by a vertical line and shows clearly that phonon wave packets are identified. The theoretical curves are the result of a simulation discussed below. This experimental arrangement realizes an extremely desirable goal for phonon physics—the ability to create phonons within a buried highly localized region of the sample, and probe their arrival at another precisely defined point, in this case, the sample surface. Through band structure engineering, these impedance-matched regions can be close enough to explore the physics of high-wave-vector

FIG. 3. Time-resolved phonon deflections for the samples of Fig. 1 on identical vertical scales. Expected LA arrival times from QW (solid) and GaAs buffer (dashed) are marked as vertical lines. The simulated curves are described in the text.
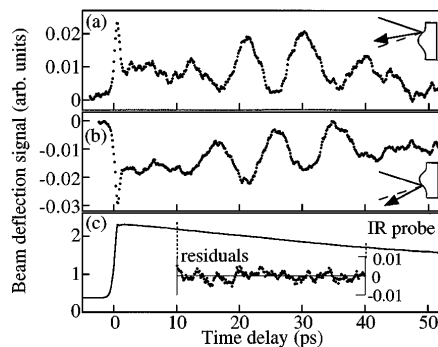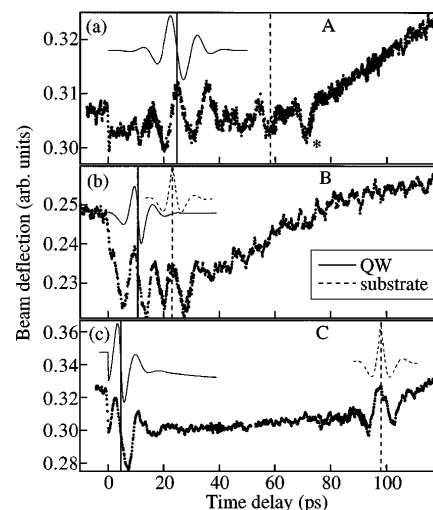
FIG. 2. Typical time-resolved deflection signals from sample A: (a) Probe beam aligned to one side of the pump focus. (b) Probe aligned to the other side—the signal is inverted. (c) An infrared probe pulse is used. Nothing is seen, even in the residual, after subtracting a fit to the dominant relaxation.

phonons before their decay and before the onset of distortions from phonon focusing. Many previous experiments in both metals [9] and bulk semiconductors [4] were restricted in the maximum emitted phonon frequency by the rapid diffusion of electrons after laser excitation. In contrast, here the electrons are confined to a precisely known localized distribution given by their QW wave function.

Several mechanisms are known to produce acoustic phonons from the relaxation of photoinjected hot carriers [1]. The conventional scenario posits ultrafast emission of longitudinal optic (LO) and interface phonons (within 200 fs) if sufficient excess electron energy is available, followed by slower acoustic phonon emission (>10 ps) to give a Fermi-Dirac carrier distribution which cools and recombines at the band edge. These processes all result in acoustic phonons since the LO phonons subsequently decay into LA and transverse acoustic (TA) products over several picoseconds [1,2,10]. Such a thermal expansion is normally invoked to explain the generation of high-frequency sound waves from picosecond optical pulses [11]; however, as discussed below, the expected delayed onset of phonon emission is not seen here. Much prompter acoustic phonon pulses can be formed via the deformation potential, acting coherently, when a high-density electron-hole plasma is deposited within the 70 fs optical pulse width. In the subsequent 100 fs, there is insufficient time for energy transfer from the electrons to the ions, but the excitation of the valence electrons and screening by the plasma weaken the interatomic bonds. The ions, which are still moving at their thermal velocities, are freer to move, and they attempt to rearrange to increase the ionic separation. The resultant increase in stress of the quantum well region launches a displacement impulse which propagates through the surrounding AlGaAs and to the surface. This mechanism can be viewed as the initial nonequilibrium contribution of the deformation potential (which is normally averaged over time, electron energy, etc.), and is strongly related to ultrafast laser-induced melting of semiconductors [12], where a large enough plasma density instantaneously destabilizes and melts the lattice without it being directly heated to its melting point. The phonon pulse in the QW can substantially alter the carrier cooling in the coherent regime (<5 ps), where the anomalous carrier dynamics is now under intense scrutiny [13]. Thus, at the earliest stages of optical excitation of a semiconductor using ultrafast pulses, the lattice is simultaneously responding to an impulse that couples not just LO phonons, but LA phonons as well.

In the present case, the acoustic phonon wave packet follows to first order the $1s$ confined electron probability density [the injected stress, $\Delta\sigma(z, t > 0) \propto |\psi_{1s}(z)|^2$] and moves out of the quantum well at the sound velocity. Thus the frequencies in the phonon pulse are tunable by suitably engineering the QW wave functions using band-structure engineering, allowing the production of phonons up to several THz. Because the acoustic impedance mismatch between the GaAs QW and the $Al_{0.3}Ga_{0.7}As$ barriers is

low, there will be little phonon confinement within the well. Using a one-dimensional elastic continuum model [11], the lattice displacement, u, is given by

$$\rho \frac{\partial^2 u(z,t)}{\partial t^2} = \rho v^2 \frac{\partial \eta(z,t)}{\partial z} - \frac{\partial \Delta\sigma(z,t)}{\partial z}, \quad (1)$$

where the stress $\Delta\sigma$ drives the strain and $\eta = \partial u/\partial z$ for sound velocity v and density ρ. This wave equation produces a unipolar strain pulse [Fig. 1(c)] if the induced stress decays slowly compared to $\tau_{exit} = d_{QW}/v$, the time taken for phonons to leave the QW. The phonon signal is smaller for the wider 250 Å QW because the resulting stress gradient driving u in Eq. (1) is weaker. The phonon wave packet is reflected by the free surface back into the sample. If the phonon deflection signal were sensitive only to the geometric bowing of the sample surface, a step change is expected when the phonons arrive. Instead, the observed oscillations indicate that a second detection mechanism dominates, due to changes in the dielectric constants within the strain field, acting as a lens. In this case the net phase of the reflected probe light must be calculated by integrating down through the penetration depth ($\zeta = \frac{\lambda}{4\pi\kappa} \sim 16$ nm for refractive index $n + i\kappa$). Following [11], we find the change in reflection coefficient,

$$\Delta r = \frac{8\pi i(n + i\kappa)}{\lambda(1 + n + i\kappa)^2}\left\{\frac{\partial n}{\partial \eta} + i\frac{\partial\kappa}{\partial\eta}\right\}$$
$$\times \int_0^\infty dz\,\eta(z)e^{-z/\zeta + 4\pi inz/\lambda},$$

and extract the relative phase as a function of time to model the induced phonon deflection. The oscillatory terms are due to interference between induced lens contributions at different depths. The solid curves in Fig. 3 show the simulation for a slowly decaying ($>\tau_{exit}$) induced stress using the photoelastic coefficients from [7]. Although the general features are reproduced, there are major discrepancies which we are unable to explain using trivial modifications. In particular, the signal in A is clearly phase shifted, and extra oscillations arrive earlier and last longer than expected from the QW width. One possible explanation, the attenuation of high-frequency phonons (here $f \lesssim 0.5$ THz) by scattering with the thermal bath is considered insignificant since the required absorption would have to be 10^3 times larger than in bulk GaAs [14], exceeding even that of amorphous glasses [15]. It is also unlikely to be from an extended probe skin depth since the falloff of the wave-packet signal remains sharply defined, and minimal attenuation is clearly seen for the phonon wave packet emitted by the underlying GaAs substrate [~ 98 ps in Fig. 3(c)]. A third possibility is the failure of the idealized phonon generation assumed here: The fits are improved by wave-packet lengths double that expected from the QW widths. Such departures from simple theory suggest the influence of nonequilibrium dynamics during the ≤ 25 nm localized phonon generation or ≤ 100 nm propagation; however, more detailed theoretical and experimental work is required.

An additional unexplained feature [at 70 ps ($*$) in Fig. 3(a)] matches the arrival of fast TA phonons propagating along [$1\bar{1}0$]. Although oriented TA phonons are seen in bolometric measurements of sub-μs phonon pulses in bulk GaAs [16], this relies on the directional selectivity of phonon focusing. We tentatively suggest that inelastic scattering of the initial high-wave-vector LO and LA phonons also selects particular orientations, as noted theoretically [17].

The rise in phonon deflection on longer time scales is due to the successive arrival of quasiballistic ($\tau_{\text{rise}} \geq \tau_{\text{ballistic}}$), quasidiffusive ($\tau_{\text{rise}}^{\text{calc}} \sim 300$ ps), and diffuse ($\tau_{\text{rise}}^{\text{calc}} \sim 4$ ns) phonons [3] transporting the heat deposited by the pump pulse in the underlying substrate (Fig. 4). This signal, previously unresolved due to unfavorable experimental geometries, contains detailed information on phonon scattering at early times. The observed rise is always coincident with the ballistic phonon pulse from the substrate (Fig. 3), implying that these phonons do not come from the QW. Because the onset of the rise immediately follows the ballistic phonons, we ascribe the first component to quasiballistic or "snake" phonons that have downconverted to yield phonon products conserving momentum (Fig. 4, inset). Detailed calculations of this nonequilibrium cascade contribution are extremely complicated [3]. Another mechanism recently invoked is rapid phonon thermalization via electron-electron scattering within the photoinjected plasma [18]. The plasma would then rapidly emit low-frequency ballistic phonons; however this is unable to account for the 300 ps rise time observed here. At later times, the quasiballistic arrivals merge with quasidiffuse and diffuse phonon transport (as given above), implying that the contribution of fully diffusive transport extends beyond the experimental time window, being detected only as the long-lived background ($\Delta T \sim 10$ K) on which the signals sit.

The absence of significant quasiballistic rise from the QW [clearly negligible in Fig. 3(c)] is surprising. It may be caused by the high radiative efficiency of the QW which returns most of the injected energy as light [19]. In contrast, nonradiative recombination in the bulk GaAs substrate generates a substantial incoherent acoustic phonon population. This also supports our thesis that the phonon wave packets emitted by the QW are caused by a coherent deformation potential which should give negligible delayed thermal rise.

In conclusion, we have developed a dual-color time-resolved surface deflection phonon spectroscopy that, in conjunction with band-gap-engineered semiconductor heterostructures, enables the generation, propagation, and detection of phonons in localized well-defined geometries. Ultrafast phonon wave packets produced in single GaAs quantum wells by a previously neglected coherent deformation-potential mechanism can be resolved as they arrive at the surface. At later times, quasiballistic snake phonons contribute to a 300 ps buildup of the surface deformation. Such experiments demonstrate the capability of quantum-confined electronic systems to probe phonon physics on short spatial and temporal scales.
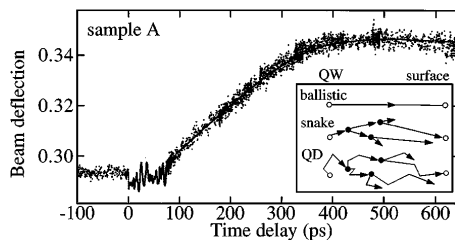
FIG. 4. Deflection signal at longer times in sample A. After the oscillations (up to 80 ps) the deflection gradually increases as the quasiballistic snake phonons arrive from the substrate. Inset: phonon trajectories—the snake phonons undergo downconversion ($\bullet$) but retain their original direction. Quasidiffuse (QD) phonons undergo more elastic scattering.

[1] For a review, see J. A. Kash and J. C. Tsang, in *Light Scattering in Solids VI,* edited by M. Cardona and G. Güntherodt (Springer-Verlag, Berlin, 1991), p. 423–518.
[2] J. J. Baumberg and D. A. Williams, Phys. Rev. B **53**, R16 140 (1996); T. Dekorsy *et al.,* Phys. Rev. B **53**, 1531 (1996), and references therein.
[3] Y. B. Levinson, in *Nonequilibrium Phonons in Nonmetallic Crystals,* edited by W. Eisemenger and A. A. Kaplyanskii, (Elsevier, Amsterdam, 1986), p. 91–144.
[4] S. A. Akhmanov and V. E. Gusev, Sov. Phys. Usp. **35**, 153 (1992).
[5] H. T. Grahn, H. J. Maris, J. Tauc, and B. Abeles, Phys. Rev. B **38**, 6066 (1988).
[6] O. B. Wright and K. Kawashima, Phys. Rev. Lett. **69**, 1668 (1992).
[7] P. Etchegoin *et al.,* Phys. Rev. B **46**, 15 139 (1992).
[8] P. Basseras *et al.,* J. Appl. Phys. **75**, 2761 (1994).
[9] G. Tas and H. J. Maris, Phys. Rev. B **49**, 15 046 (1994).
[10] M. Giltrow *et al.,* Phys. Rev. Lett. **75**, 1827 (1995).
[11] C. Thomsen, H. T. Grahn, H. J. Maris, and J. Tauc, Phys. Rev. B **34**, 4129 (1986).
[12] P. Stampfli and K. H. Bennemann, Phys. Rev. B **49**, 7299 (1994).
[13] *Coherent Optical Interactions in Semiconductors,* edited by R. T. Phillips, NATO ASI (Plenum, New York, 1994).
[14] W. Chen, H. J. Maris, Z. R. Wasilewski, and S. Tamura, Philos. Mag. B **70**, 687 (1994).
[15] T. C. Zhu, H. J. Maris, and J. Tauc, Phys. Rev. B **44**, 4281 (1991).
[16] M. T. Ramsbey, S. Tamura, and J. P. Wolfe, Phys. Rev. B **46**, 1358 (1992).
[17] A. Berke, A. P. Mayer, and R. K. Wehner, J. Phys. C **21**, 2305 (1988).
[18] M. E. Msall, S. Tamura, S. E. Esipov, and J. P. Wolfe, Phys. Rev. Lett. **70**, 3463 (1993).
[19] C. Weisbuch and B. Vitner, *Quantum Semiconductor Structures* (Academic, London, 1991), p. 170.